Electronic Supplementary Material (ESI) for Journal of Materials Chemistry A.

Electronic supplementary information (ESI) for

The influence of the variation in preferred orientation of tin sulfide absorbers on the performance of thin-film solar cells

Dajeong Lee,[a#] Jae Yu Cho,[a#] Hee-Sun Yun,[bc] Doh-Kwon Lee,[bc] Taehoon Kim,[d] Kijoon Bang,[e] Yun Seog Lee,[df] Ho-Young Kim[df] and Jaeyeong Heo[a]*

[a]Department of Materials Science and Engineering, and Optoelectronics Convergence Research Center, Chonnam National University, Gwangju 61186, Republic of Korea

[b]Photo-electronic Hybrids Research Center, Korea Institute of Science and Technology (KIST), Seoul 02792, Republic of Korea

[c]Division of Nano and Information Technology, KIST school Korea University of Science and Technology, Seoul 02792, Republic of Korea

[d]Department of Mechanical and Aerospace Engineering, Seoul National University, Seoul 08826, Republic of Korea

[e]Global Frontier Center for Multiscale Energy Systems, Seoul National University, Seoul 08826, Republic of Korea

[f]Institute of Engineering Research, Seoul National University, Seoul 08826, Republic of Korea

[#]These authors contributed equally to this work.

*E-mail: jheo@jnu.ac.kr

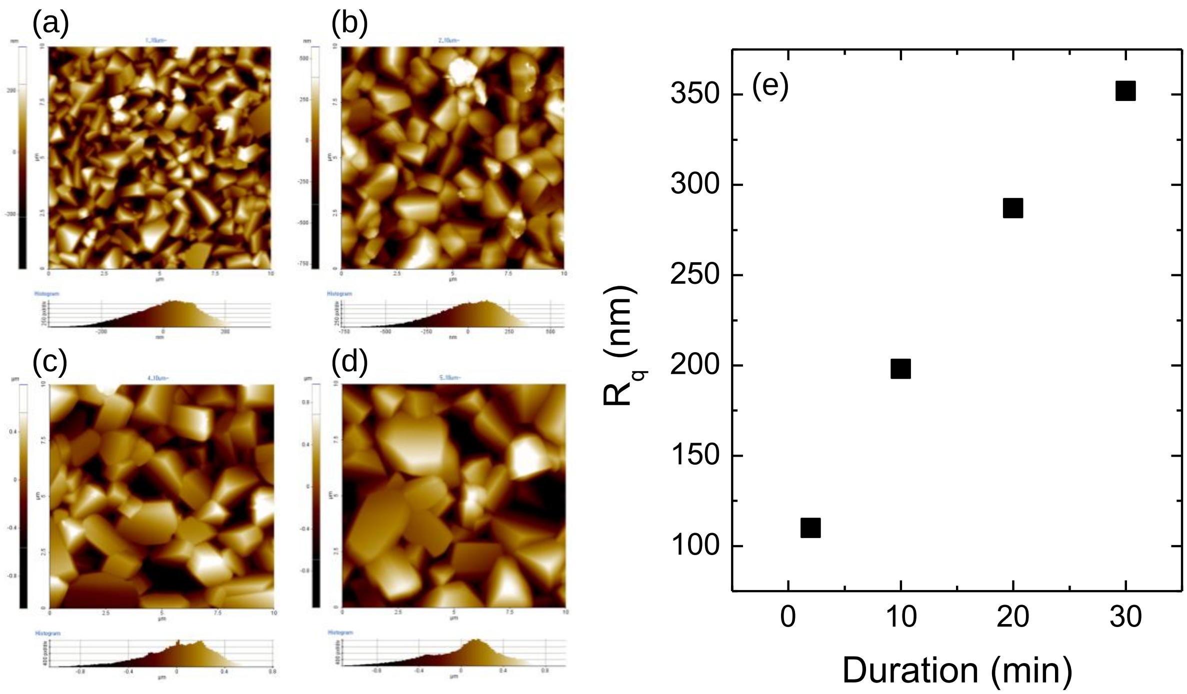

Fig. S1 AFM images of SnS absorbers grown at various durations of (a) 2 min, (b) 10 min, (c) 20 min, and (d) 30 min. Here, the image size is 10 µm × 10 µm. (e) Root-mean-square roughness (R_q) of SnS absorbers.

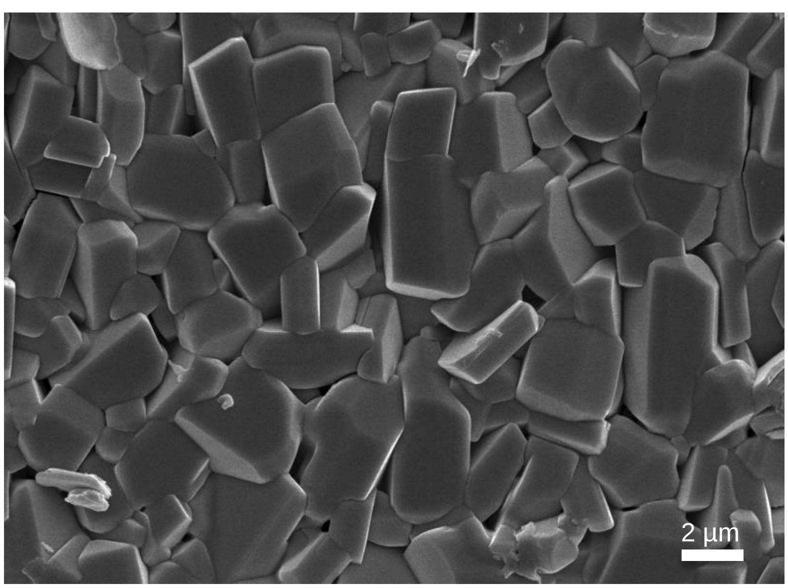

Fig. S2 Plane-view SEM image of SnS absorber grown for 40 min.

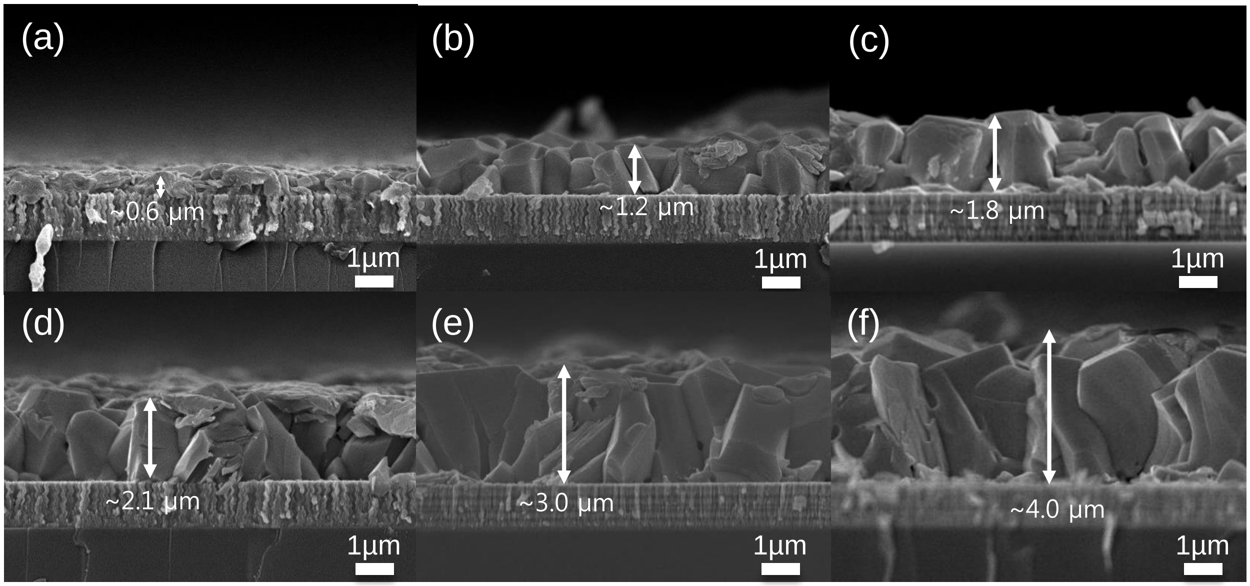

Fig. S3 Cross-sectional SEM images of SnS grown for (a) 2 min, (b) 10 min, (c) 15 min, (d) 20 min, (e) 30 min, and (f) 40 min, respectively.

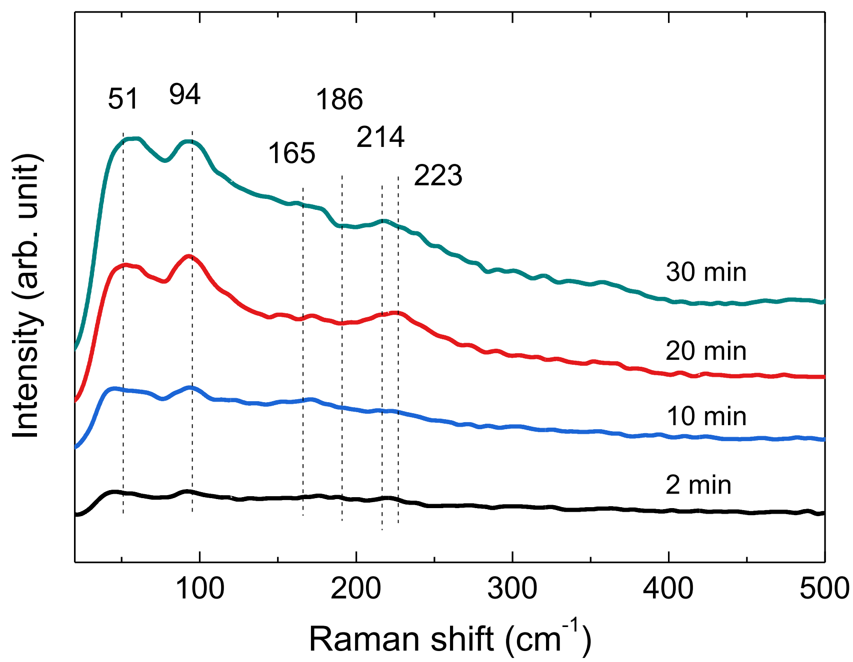

Fig. S4 Raman spectra for the SnS absorbers at different growth durations from 2 to 30 min.

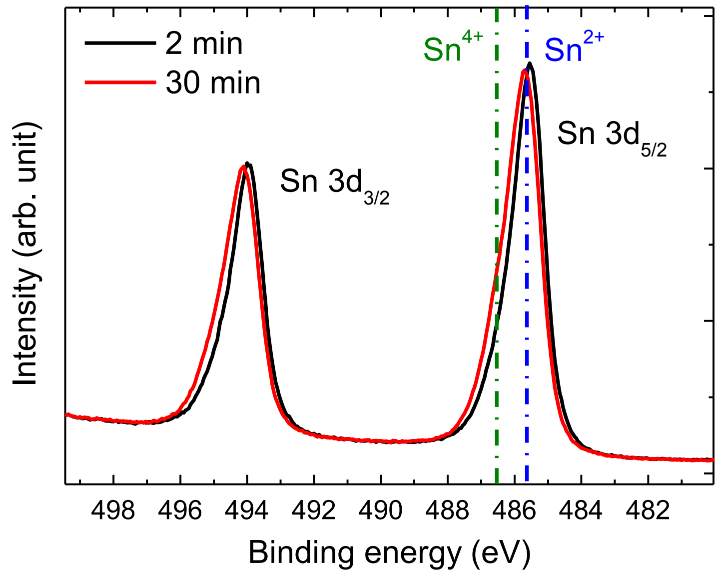

Fig. S5 XPS Sn 3d spectra for SnS absorbers grown for 2 min and for 30 min after surface Ar^{+} cleaning. Binding energy of 485.6 and 486.5 eV correspond to Sn^{2+} and Sn^{4+}, respectively.[R1] Chemical state of Sn for both films is mainly Sn^{2+}.

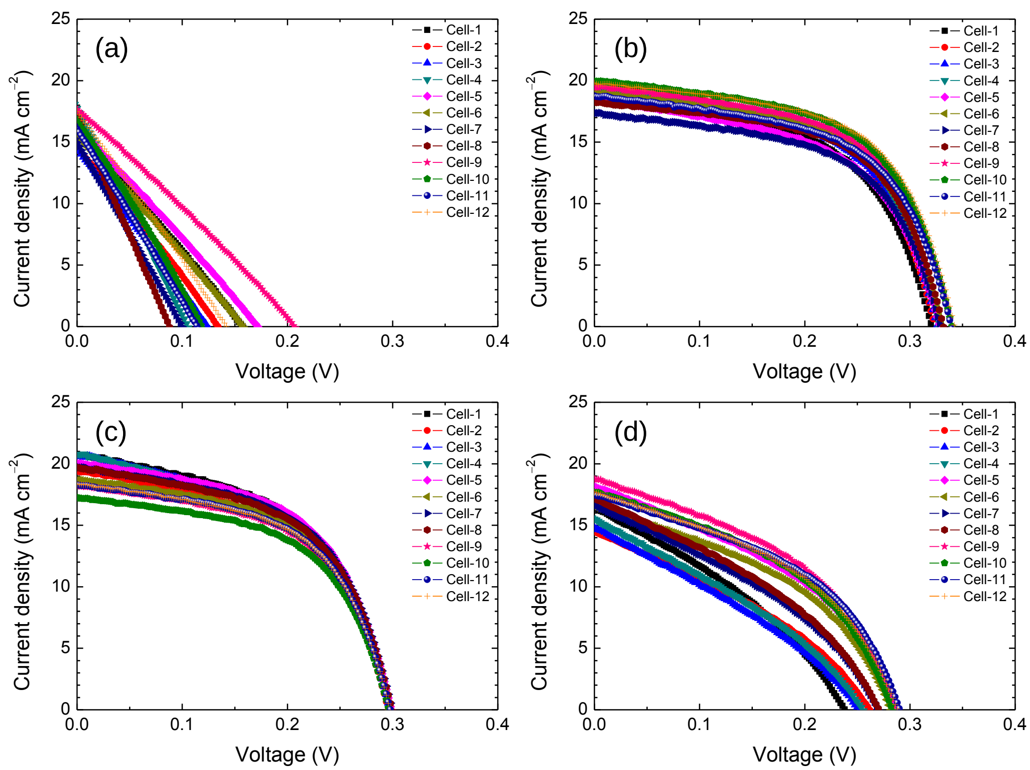

Fig. S6 All the *J*–*V* characteristics of the four SnS TFSC samples containing 12 cells each with different growth durations of (a) 2 min, (b) 10 min, (c) 20 min, and (d) 30 min.

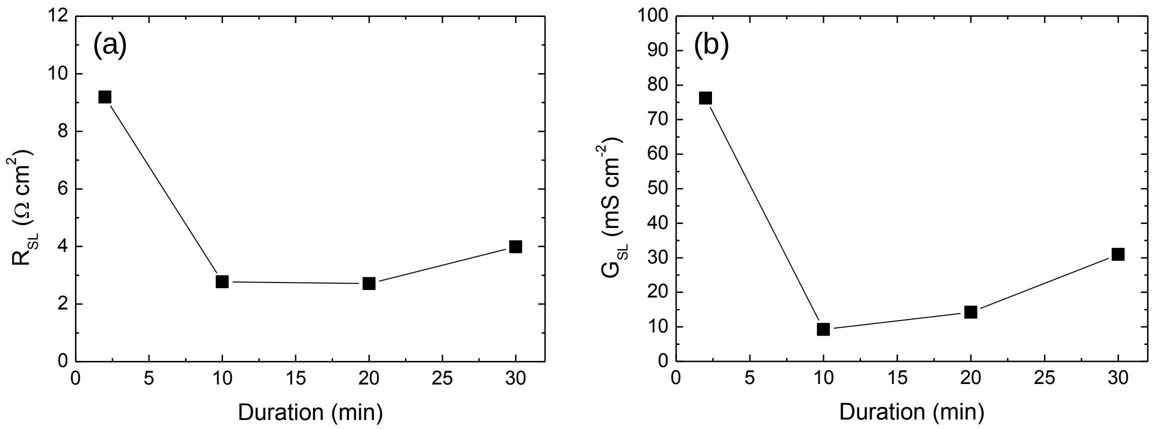

Fig. S7 (a) Series resistance (R_{SL}) and (b) shunt conductance (G_{SL}) under light for the devices shown in Fig. 6(a).

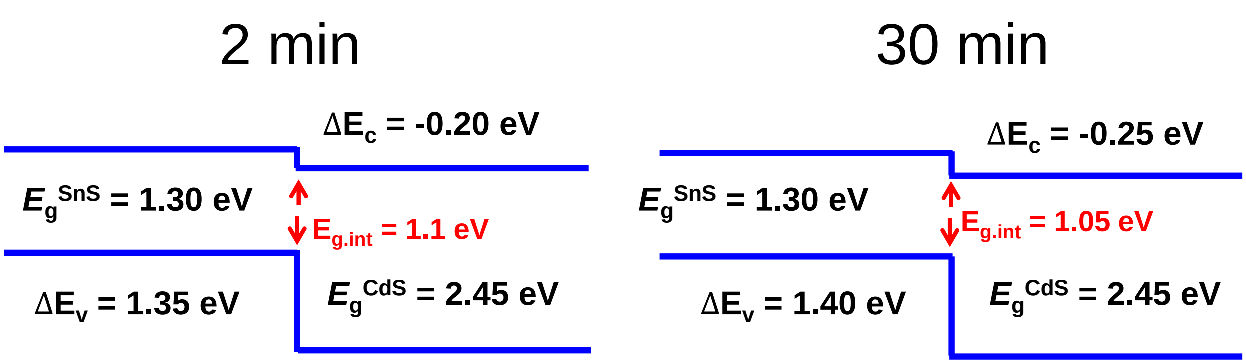

Fig. S8 Schematic for the measured band structure of 2-min and 30-min SnS absorbers with CdS buffer using Kraut method.[R2]

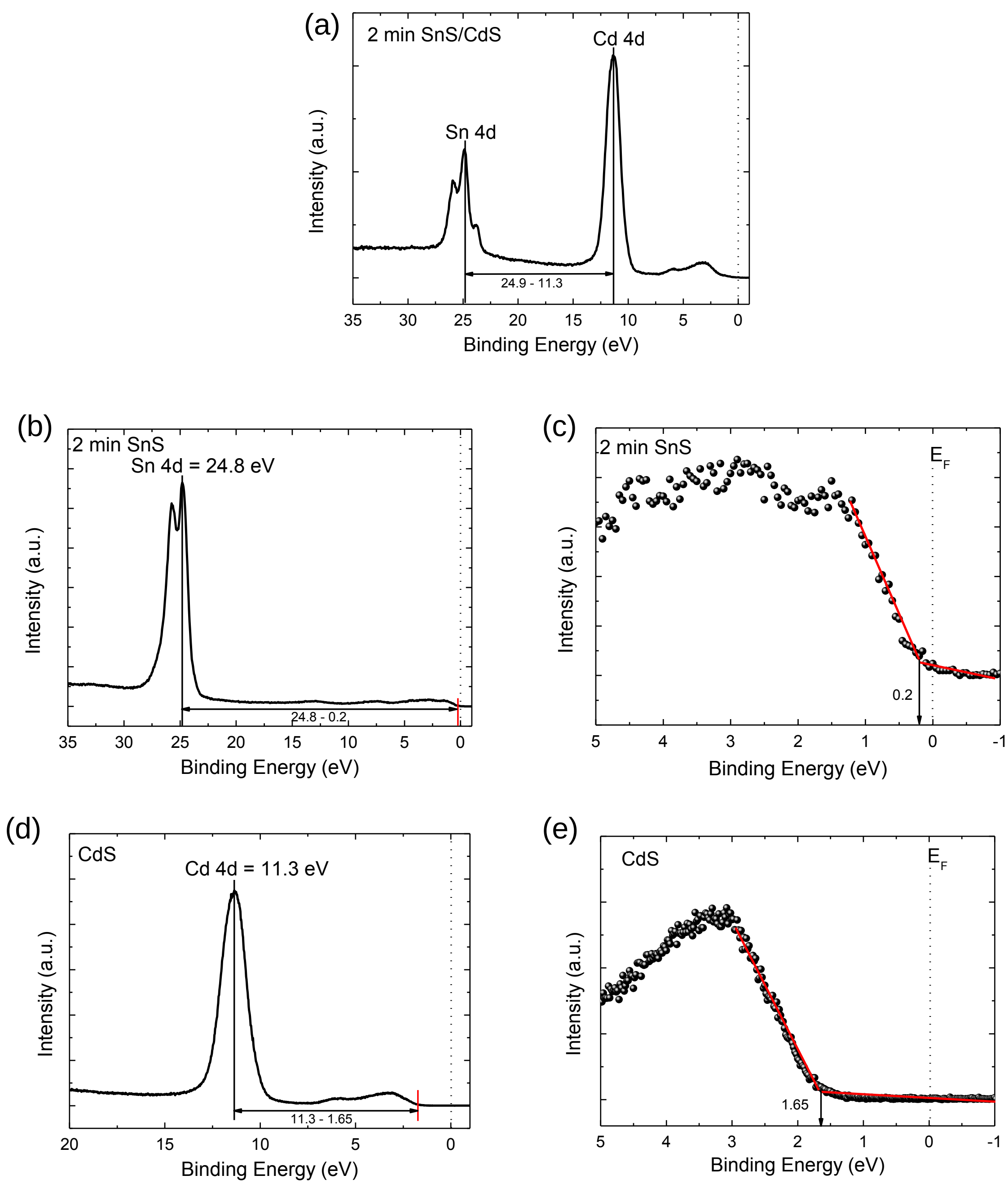

Fig. S9 (a) XPS Sn 4d and Cd 4d peaks on etched 2-min SnS/CdS interface. (b) Sn 4d and (c) valence band on 2-min SnS sample. (d) Cd 4d and (e) valence band on CdS sample.

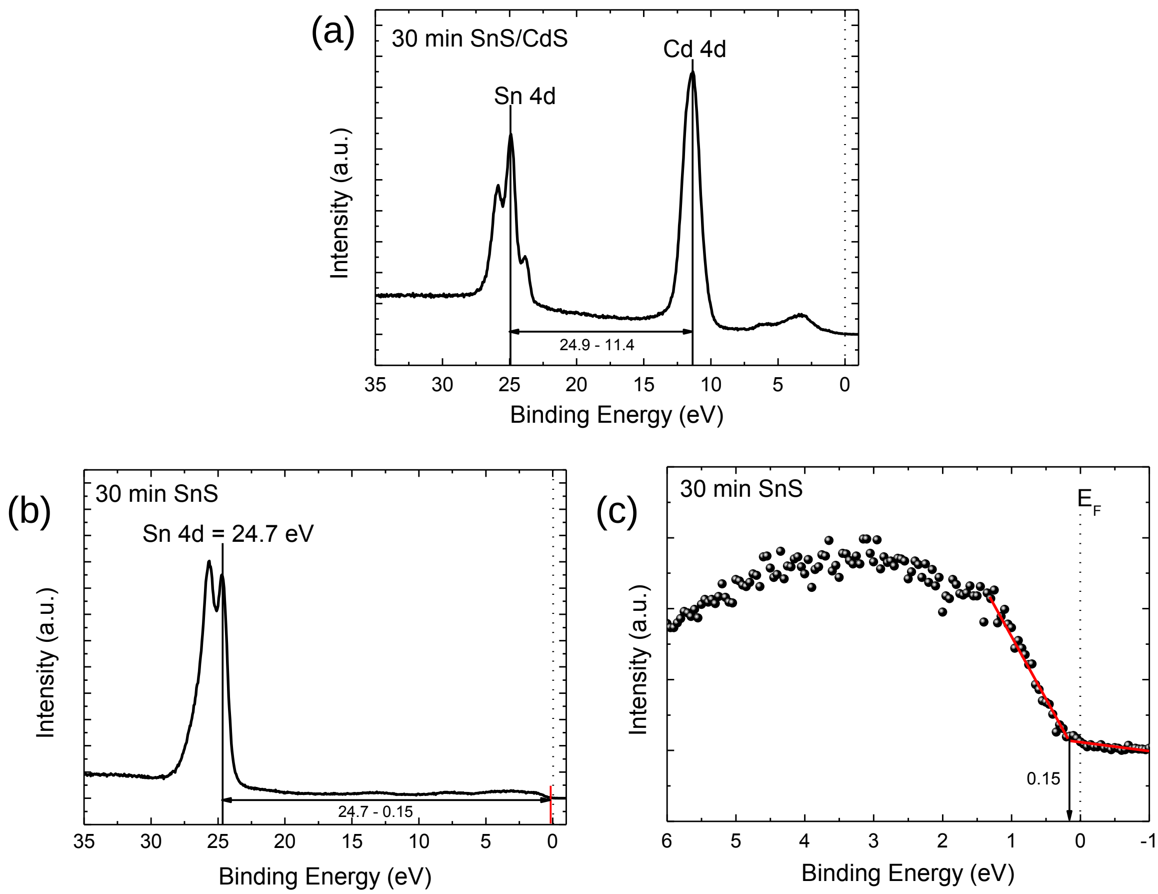

Fig. S10 (a) XPS Sn 4d and Cd 4d peaks on etched 30-min SnS/CdS interface. (b) Sn 4d and (c) valence band on 30-min SnS sample.

XPS measurements: XPS measurement was performed (Kratos, AXIS-Nova Ultra DLD). The X-ray source was monochromated Al-Kα (1486.68 eV) with binding energy calibration. Three samples were prepared: SnS grown on SLG/Mo substrate, CdS grown on FTO substrate, and SLG/Mo/SnS/CdS. In the case of SLG/Mo/SnS/CdS, depth profiling was carried out by 10 KeV Ar^+ ions until the Sn peak was detected. Valence band offset was calculated by using the following formula[R2]:

$$\Delta E_V = E_V^{SnS} - E_V^{CdS} = (E_{Sn\,4d}^{SnS-CdS} - E_{Cd\,4d}^{SnS-CdS}) - (E_{Sn\,4d}^{SnS} - E_V^{SnS}) + (E_{cd\,4d}^{CdS} - E_V^{CdS})$$

where subscription and superscription mean the detected XPS peak and the used sample, respectively.

First, the 2-min SnS/CdS band offset was calculated (see Fig. S9). $E_{Sn\,4d}^{SnS-CdS}$ - $E_{Cd\,4d}^{SnS-CdS}$ was calculated to be 13.6 eV (i.e., 24.9 eV–11.3 eV). $E_{Sn\,4d}^{SnS}$ - E_V^{SnS} was measured to be 24.6 eV (i.e., 24.8 eV–0.2 eV). $E_{cd\,4d}^{CdS}$ - E_V^{CdS} was 9.65 eV (i.e., 11.6 eV–1.65 eV). Therefore, ΔE_V was -1.35 eV.

Finally, the conduction band offset (ΔE_C) was calculated using the bandgap values of SnS (1.30 eV) and CdS (2.45 eV) estimated from external quantum efficiency.

$$\Delta E_C = \left(E_g^{CdS} - E_g^{SnS} \right) + \Delta E_V$$

ΔE_C was determined to be -0.2 eV.

Second, the 30-min SnS/CdS band offset was calculated (see Fig. S10). $E_{Sn\,4d}^{SnS-CdS}$ - $E_{Cd\,4d}^{SnS-CdS}$ was calculated to be 13.5 eV (i.e., 24.9 eV–11.4 eV). $E_{Sn\,4d}^{SnS}$ - E_V^{SnS} was measured to be 24.55 eV (i.e., 24.7 eV–0.15 eV). $E_{cd\,4d}^{CdS}$ - E_V^{CdS} was 9.65 eV (i.e., 11.6 eV–1.65 eV). Therefore, ΔE_V was -1.40 eV.

Finally, the conduction band offset (ΔE_C) was calculated using the bandgap values of SnS (1.30 eV) and CdS (2.45 eV) estimated from external quantum efficiency.

$$\Delta E_C = \left(E_g^{CdS} - E_g^{SnS} \right) + \Delta E_V$$

ΔE_C was determined to be -0.25 eV.

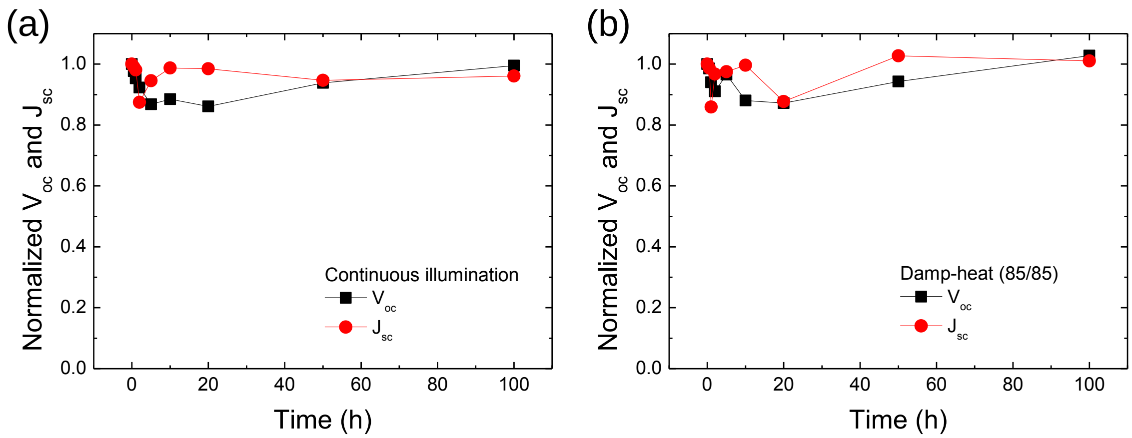

Fig. S11 Normalized V_{oc} and J_{sc} as a function of time for (a) continuous illumination and (b) damp-heat (85/85) conditions, respectively.

Table S1 Detailed cell parameters for TFSCs with different SnS growth duration. The cell with the highest efficiency for each sample is highlighted in bold with purple background.

Sample	V_{oc} (V)	J_{sc} (mA cm^{-2})	**FF**	η (%)	R_{SL} (ohm cm^{2})	G_{SL} (mS cm^{-2})
2 min	0.157	15.7	0.264	0.654	9.1	96.5
	0.134	14.5	0.268	0.521	8.4	102.5
	0.124	14.5	0.26	0.466	7.8	110.3
	0.105	17.7	0.256	0.479	5.5	163.8
	0.172	16.2	0.265	0.734	10.0	85.0
	0.158	15.5	0.259	0.634	10.0	91.0
	0.100	15.0	0.253	0.378	6.7	145.0
	0.088	17.0	0.254	0.380	4.6	185.8
	0.207	**17.6**	**0.269**	**0.981**	**9.2**	**76.3**
	0.119	16.7	0.273	0.54	16.7	118.8
	0.114	16.1	0.257	0.473	6.0	132.0
	0.142	17.5	0.259	0.645	15.4	113.0
Average	0.135	16.2	0.261	0.574	9.1	118.3
10 min	0.321	19.1	0.531	3.25	3.1	11.8
	0.326	19.7	0.548	3.52	5.7	10.8
	0.326	18.4	0.576	3.46	3.0	4.3
	0.328	19.3	0.573	3.62	3.0	1.8
	0.329	18.6	0.53	3.23	3.1	9.3
	0.331	19.0	0.57	3.59	2.7	8.0
	0.329	17.4	0.564	3.22	3.3	4.0
	0.332	18.3	0.578	3.50	2.9	12.0
	0.340	19.5	0.564	3.73	2.9	3.8
	0.340	20.0	0.569	3.86	2.7	6.5
	0.340	18.8	0.561	3.57	2.9	6.0
	0.342	**19.8**	**0.58**	**3.93**	**2.8**	**9.3**
Average	0.332	19.0	0.562	3.54	3.2	7.3

20 min	0.299	20.8	0.522	3.24	2.9	13.0
	0.296	19.4	0.519	2.98	3.0	16.8
	0.298	20.6	0.511	3.13	2.9	12.0
	0.298	20.8	0.5	3.10	3.0	24.5
	0.299	**20.0**	**0.546**	**3.26**	**2.7**	**14.3**
	0.298	18.7	0.546	3.04	3.1	18.0
	0.299	19.7	0.543	3.21	2.8	11.5
	0.300	19.7	0.538	3.17	3.0	12.8
	0.299	18.2	0.544	2.96	3.2	8.8
	0.296	17.3	0.548	2.81	3.0	6.0
	0.298	18.3	0.55	3.00	3.1	12.0
	0.298	18.3	0.549	2.99	3.0	9.8
Average	0.298	19.3	0.535	3.07	3.0	13.3
30 min	0.238	16.5	0.334	1.31	6.0	42.0
	0.262	14.5	0.339	1.28	7.8	38.5
	0.252	14.8	0.311	1.16	8.7	41.0
	0.255	15.5	0.318	1.26	8.3	48.3
	0.288	18.2	0.398	2.08	4.8	31.3
	0.282	16.5	0.414	1.93	5.4	24.5
	0.270	16.7	0.351	1.58	6.1	41.0
	0.270	17.2	0.355	1.65	5.7	41.5
	0.287	**18.8**	**0.429**	**2.31**	**4.0**	**31.0**
	0.283	17.7	0.427	2.14	4.3	27.5
	0.290	17.5	0.436	2.21	4.3	23.8
	0.288	17.7	0.421	2.15	4.5	28.0
Average	0.272	16.8	0.378	1.76	5.8	34.9

References for ESI

R1 T. J. Whittles, L. A. Burton, J. M. Skelton, A. Walsh, T. D. Veal and V. R. Dhanak, *Chem. Mater.*, 2016, **28**, 3718–3726.

R2 R. E. Brandt, M. Young, H. H. Park, A. Dameron, D. Chua, Y. S. Lee, G. Teeter, R. G. Gordon and T. Buonassisi, *Appl. Phys. Lett.*, 2014, **105**, 263901.